Dynamic Behavior of Confined Branched Hydrocarbon Lubricant Fluids under Shear

Carlos Drummond and Jacob Israelachvili*

Department of Chemical Engineering, Materials Department, and Materials Research Laboratory, University of California, Santa Barbara, California 93106

Received November 29, 1999; Revised Manuscript Received April 6, 2000

ABSTRACT: We have measured the friction forces between molecularly smooth mica surfaces confining thin films of different branched hydrocarbons, using the surface forces apparatus (SFA). The evolution of the systems to steady-state sliding from rest or after a change in sliding velocity was thoroughly studied, and the presence of different length and time scales was observed. Using a new "extended bimorph slider" which allows continuous shearing for distances well beyond the contact diameter, we show that the evolution to steady-state sliding in these films is governed by the distance the surfaces are sheared rather than the time. From these results it is clear that both time and distance of sliding have to be considered in order to fully describe the dynamic response of lubricants and complex fluids under shear.

Introduction

The frictional forces between sliding surfaces appear in many problems in physics and engineering. From earthquake studies to precise control of moving parts or data storage technology, frictional stresses play a fundamental role not completely understood in most cases, even though the problem is one of the oldest in physics. It is not unusual to find similar equations with different names in very different fields, aiming to describe phenomena that are basically the same. Da Vinci, Coulomb, Euler, Amontons, and many others were attracted to this problem: most of the experimental observations, collectively known as Amontons' laws, were originally discovered by Da Vinci two centuries before, with some of these "laws" still widely used today.[1] The study of friction has proven to be extremely complicated, mainly because the results, e.g. the friction forces, depend on many variables that cannot always be measured or controlled. As a consequence, a fundamental understanding of the origin of frictional forces and a complete characterization of the behavior of surfaces or confined liquids under shear have remained elusive. However, during the past 20 years the emergence of more sophisticated techniques, both experimental and theoretical, have allowed for deeper and more fundamental studies of tribological systems to be made. The surface forces apparatus,[2] lateral or atomic force microscopy,[3] and quartz crystal microbalance[4] experiments, together with extensive molecular dynamics simulations,[5] have set the framework for a much better understanding of the behavior of surfaces and fluids under shear.

The surface forces apparatus (SFA) has proven to be an excellent tool for investigating tribological systems. It allows the study of single or multiple asperity contacts, where the load, contact area, and sliding velocity between the surfaces can be controlled and unambiguously measured with higher accuracy than in any conventional tribometer. Furthermore, an image of the surfaces in contact can be obtained as the surfaces are slid, allowing the monitoring of the real size and shape of the contact area and the distance or film thickness profile between the surfaces when atomically smooth surfaces are used. It is relatively simple to perform a comprehensive exploration of the full parameter space to identify the variables that determine the frictional behavior of the system.

Every property measured is influenced in one way or another by the experimental setup used; this is especially important in friction force measurements which are always indirect, viz., they do not directly measure the actual or instantaneous friction force at the interface. To measure the friction force between two rubbing objects, it is necessary to couple the shearing surfaces to a compliant element—which may be the material of the surfaces themselves—whose deformation will indicate the resistance to the sliding. In the SFA this is done by driving one of the surfaces at constant velocity, V, while the other is attached to a spring that is fixed at the other end. The equivalent mechanical model of the apparatus is shown in Figure 1. From the deflection of the spring of known spring constant (K), the position (x) of the center of mass of the upper surface is determined, and the friction force between the surfaces (F_f) can be calculated using

$$m\ddot{x} = K(x - x_0) + F_f \tag{1}$$

where m is the mass of the upper surface, and $(x - x_0)$ is the deflection of the spring from its equilibrium length. As can be inferred from eq 1, mechanical properties of the measurement system (e.g., compliance and inertial mass) will influence the results; these factors have to be taken into account in order to obtain meaningful information from the convoluted signal. This can be done in a straightforward fashion in the SFA because of its mechanical simplicity and easy-to-characterize mechanical properties. If the inertial term $m\ddot{x}$ in eq 1 can be neglected, the force between the surfaces can be obtained directly from the deflection of the spring. This is actually the case for the experiments reported in this paper.

Many different systems have been studied in the past 10 years using either the SFA or the other probes mentioned before. From simple quasi-spherical molecules[6−10] and short hydrocarbon chains[6,7,11] to polymers and

10.1021/ma9919918 CCC: $19.00
Published on Web 06/02/2000

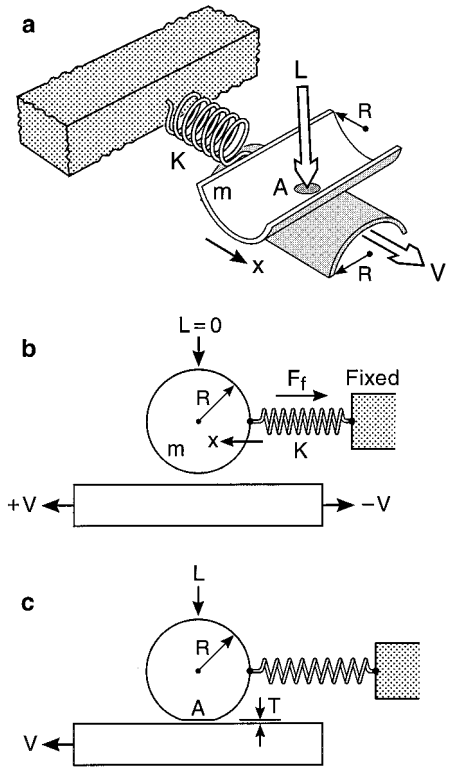

Figure 1. Schematic geometry of the friction experiments with the surface forces apparatus (SFA). When the two mica surfaces are pressed into contact under a normal load *L*, the glue layer used to attach the mica to the silica lenses of radii *R* undergoes elastic deformation. A circular contact area *A* confines a thin film of thickness *T*. The lower surface is driven laterally at velocity *V*. The friction force between the two surfaces induces lateral movement in the upper surface of mass *m*, which is attached to a displacement sensing or friction-force measuring spring of stiffness *K*. All of these factors determine the friction force *F* measured by the spring. The equivalent sphere-on-a-plate geometry is also presented.

mixtures,[12−19] systems of increasingly complexity have been the subjects of scrutiny of many research groups. In this paper we report on results obtained with three lubricant fluids of intermediate complexity that serve as model systems for typically used base lube oils. Our new experimental setup allows continuous shearing of the surfaces for distances much longer than the typical contact size, revealing some very interesting characteristics of the friction phenomenology not completely appreciated in the past.

Experimental Section

The experiments described in this paper were realized with an SFAIII modified for friction studies, which has been described elsewhere.[20] Back-silvered molecularly smooth mica surfaces are glued to cylindrically curved silica lenses and are used to confine liquid films of the lubricants under study. The lower surface is mounted on a bimorph slider,[14] which moves laterally in linear fashion when a constant slope voltage ramp is applied between its two electrodes. The upper surface is attached to a vertical double cantilever spring whose deflection is monitored using semiconductor strain gauges. In this way, the friction force between the surfaces induced by the displacement of the lower surface can be measured with an accuracy of 0.01 mN. The cylindrically shaped silica disks are placed with their axes perpendicular to each other. If the separation between the curved surfaces is much smaller than their radii of curvature, *R*, this configuration is equivalent to a sphere-on-plate contact, as shown in Figure 1. When the mica surfaces are brought into contact under a controlled load, *L*, the glue layer under the surfaces undergoes elastic deformation, and the thin lubricant films are confined to a circular region of uniform thickness *T* and area *A*.

Table 1

lubricant	formula	viscosity [cP]	characteristics
squalane	$C_{30}H_{62}$	6	monodisperse, 6 methyl side groups
PAO	$C_{46}H_{94}$	6	4-arm star-shaped
Exxsyn	mixture	6	mixture of branched hydrocarbons

Multiple beam interferometry[21] (MBI) was used to monitor the distance between the surfaces and the geometry of the contact in real time. The separation between the surfaces, *T*, could be measured with an accuracy of 0.1 nm, and the area of contact, *A*, could be determined with a relative error of 10% by observing the flat region on the fringes of equal chromatic order (FECO). From the shape of the FECO, any wear or damage of the surfaces can be easily detected as soon as it occurs,[21] allowing one to distinguish between undamaged sliding and friction with wear. All the results reported in this paper were obtained with atomically smooth undamaged mica surfaces (wearless friction).

We studied thin films of three complex branched hydrocarbon lubricant fluids provided by Exxon Lube Technology Research Division: 2,6,10,15,19,23-hexamethyltetracosane (squalane), poly-α-olefin, PAO (4-arm star-shaped molecule, pentamer of decene), and Exxsyn (a mixture of branched hydrocarbons, similar to some base lube oils). Some properties of the lubricants studied are listed in Table 1. The liquids were filtered with a membrane of pore size 0.25 μm before being used to remove undesired particles; otherwise, they were used as received. Prior to injecting a lubricant droplet between two clean mica surfaces, the apparatus was purged with dry nitrogen gas for 8 h. After injecting a 100 μL drop of the lubricant between the mica surfaces, a small amount of phosphorus pentoxide (P_2O_5) was placed inside the sealed apparatus chamber to maintain dry conditions throughout the experiment. The system was allowed to thermally equilibrate (typically 2−3 h) prior to every experiment. The temperature was controlled within 0.1 °C.

Results

Steady-State Sliding: Smooth and Stick−Slip Regimes. When these lubricant films were subjected to shear, very rich dynamic behavior was observed. In general, two very distinct dynamic regimes were found: at higher velocity, *V*, the sliding is relatively smooth, i.e., the friction force measured is constant (there is no stick−slip), but with small fluctuations around an average value. On the other hand, when the velocity of sliding is slower than a given critical velocity, V_c, the friction force oscillates between two values, which are generally referred to as the "static" and "kinetic" friction forces, in a very regular way. A slow "stick" period (with the two surfaces moving almost at the same speed) is followed by a very fast "slip", until the surfaces restick.

Friction traces for the different conditions are reproduced in Figure 2. The value of the critical velocity V_c strongly depends on the load, temperature, and the mass *m* and stiffness *K* of the system, as has been analyzed before.[22] In general, it was observed that V_c increases with increasing temperature, decreasing load, and decreasing stiffness of the spring used to measure the friction force. A higher critical velocity was found for thin films of squalane compared to that of PAO, and with the experimental setup utilized (*K* between 500 and 2000 N/m), no stick−slip friction was observed for thin films of Exxsyn, suggesting that its V_c—if one exists—is even lower than that of PAO.

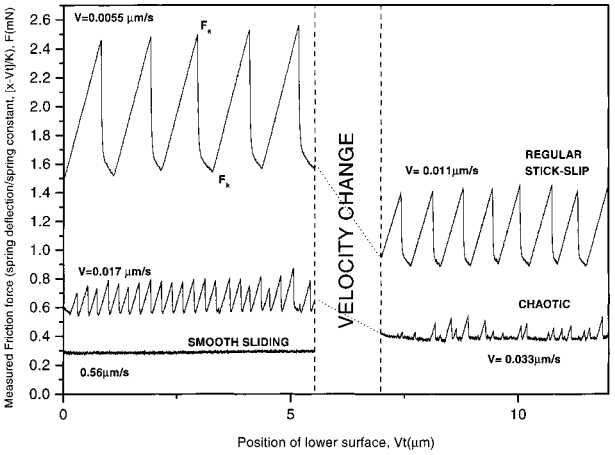

Figure 2. Actual friction traces obtained at different sliding velocities, V, for squalane thin films, at $L = 1.5$ mN, $K = 1900$ N/m, and $T = 26$ °C.

Stick−slip to smooth-sliding transitions that appear to be abrupt or "discontinuous" have been previously observed for many different systems; however, the three liquids studied here appear to show a "continuous" transition with increasing velocity, as can be observed in Figure 2. There is a velocity regime where the films do not clearly show either stick−slip or smooth-sliding characteristics, where apparently random bursts of stick−slip events can be followed by a period of relative calm, until eventually a new stick−slip event emerges. The transition regime seems to be chaotic rather than random. In this sense, trying to determine a precise value for V_c may be misleading. In addition, these thin films can become trapped in metastable states.

The transition observed for these films therefore differs significantly from what has been observed in the past for simpler liquids, such as spherical molecules and linear hydrocarbons, which show a discontinuous first-order transition.[7,13,23] On the other hand, a continuous transition was reported for slightly branched hydrocarbon thin films.[7] In this paper, we describe the details of the friction force dynamics in the quasi-smooth sliding phase. A detailed theoretical analysis of the stick−slip to smooth sliding transition for these systems will be reported elsewhere.

Since the main purpose of this work was to study the dynamics of these liquids, we investigated their tribological response to changes in sliding velocity, load, and temperature. For this purpose, two types of experiments were conducted: stop−start and sudden change of shear rate experiments.

Stop−Start Experiments: Latency Times and Stiction Forces. In these experiments, the thin film under study is subjected to shear at a certain rate until steady-state sliding is reached. Keeping the film under confinement, the shear is stopped for a given amount of time and then resumed at the same or different shear rate; the evolution of the friction force is followed through the whole process. To obtain meaningful results, special care has to be given to controlling and measuring all the relevant experimental parameters, specially stress (normal and tangential), temperature, velocity, and stopping times. When the film is kept at rest for a time longer than a characteristic "latency time", τ_0, a peak in the friction force is typically observed when the sliding is resumed, as has been reported before.[11,12,24] This peak in the friction force is called a stiction spike, or static friction, F_s. One example of what is typically observed is presented in Figure 3a.

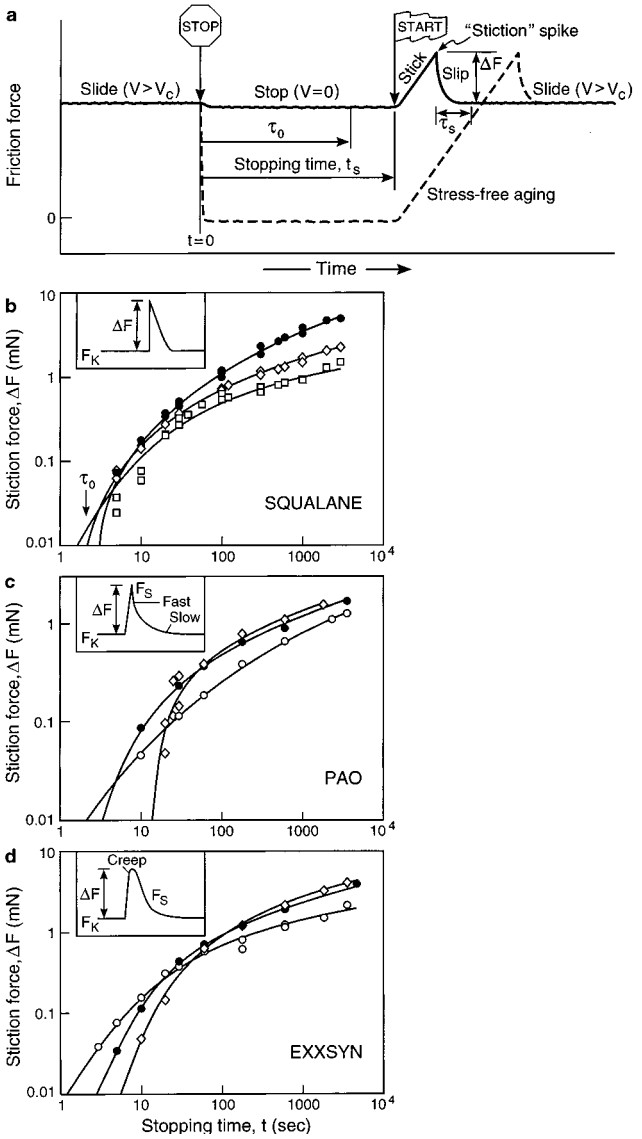

Figure 3. (a) Schematic friction trace obtained in a stiction experiment. The surfaces are held at rest for a stopping time, t_s, before resuming the sliding. The stiction force, $\Delta F = (F_s - F_k)$, is defined as the difference between the maximum recorded force F_s and the steady-state friction force, F_k. (b, c, d) Stiction forces as a function of stopping time at different loads L for thin films of squalane, PAO, and Exxsyn, respectively. Sliding velocity $V = 0.65$ μm/s. $T = 26$ °C. The insets show the typical stiction spike shapes (force−time profiles).

Figure 3 shows the values obtained for the stiction spikes for the three fluids studied as a function of stopping or waiting time at different loads. In these experiments the shear stress was allowed to relax freely after stopping the movement of the driver ($V \rightarrow 0$). Only a partial relaxation of the shear stress is typically observed once the sliding is stopped, as reported by Gee et al.[12] for different systems. On restarting, the shear rate was the same as before stopping.

The stiction spike shows a continuous and logarithmic growth with waiting time, once the latency time τ_0 is exceeded. A similar growth of F_s with contact time has been reported for many different types of systems: multiple asperity contacts of rocks,[25,26] paper,[27] and rough polymer surfaces[28] show the same general be-

havior. Yamada et al.[24] reported similar results for fluorocarbon monolayers, and Hirz et al.[29] reported similar behavior for thin films of a perfluoropolyether. Interestingly, results for simpler liquids and *n*-alkanes seem to show a different behavior: Yoshizawa and Israelachvili[11] reported an all-or-none behavior for the stiction spikes in thin films of hexadecane, with a decrease in the stiction spike height observed when the load is increased. Carlson and Berman[23] observed similar results for thin films of tetradecane.

Given that the static friction forces in Figure 3 increase in a continuous fashion, the determination of the latency time τ_0 is somehow subjective. We cannot measure a stiction spike if $\Delta F = (F_s - F_k)$ is smaller than our detection limit (around 10 μN) which can very well be the case at the shortest waiting times. Nevertheless, we can still measure upper bounds for the latency times and establish meaningful comparisons between the different systems studied. The observed latency times were longer for films of Exxsyn and PAO than for squalane. In addition, the stiction peaks were higher for thin films of squalane and significantly smaller for PAO. This indicates that the time evolution of confined thin films of squalane is significantly faster than for the other two fluids. This is not a surprising result: squalane molecules are smaller and have a simpler structure than either PAO or Exxsyn molecules. These results are also consistent with the transition to stick−slip friction being observed at higher velocities for squalane than for PAO or Exxsyn, when all the other experimental conditions (spring stiffness, load, and temperature) are the same.

The latency time also depends on load and temperature. As can be observed in Figure 3, τ_0 increases with increasing load, the same trend as observed when the temperature is reduced. Similar behavior was observed by Yamada and Israelachvili[24] for fluorocarbon surfactant monolayers and by Yoshizawa and Israelachvili[11] for thin films of *n*-hexadecane.

The shear stress applied to the films as they age during the stopping period also has an effect on the static friction force F_s or ΔF measured on restarting. Different values are obtained when the films are aged under a finite shear stress compared to stress-free conditions. Figure 4 shows the stiction spikes observed for thin films of squalane and PAO aged under both conditions. As can be seen, the stiction spikes measured when the lubricant is kept under a finite tangential force are consistently lower than for stress-free aging. These results seem to indicate a correlation between the static force and the degree of alignment of the molecules in the shear direction. It is reasonable to expect longer "randomization times" when the films are maintained under a finite stress compared with stress-free aging because of the presence of a driving force compelling the molecules to remain aligned. In other words, it will be easier for the molecules to adopt a more disordered configuration under stress-free conditions, thereby increasing the static friction force more quickly. A somehow different result is reported by Berthoud et al.,[28] who also recognized the importance of controlling the shear stress during the resting period. In their study of rough, unlubricated surfaces of both polystyrene and PMMA, they found that in general the static friction is substantially *lower* when the surfaces are aged under stress-free conditions, contrary to what we observed for smooth, lubricated contacts.

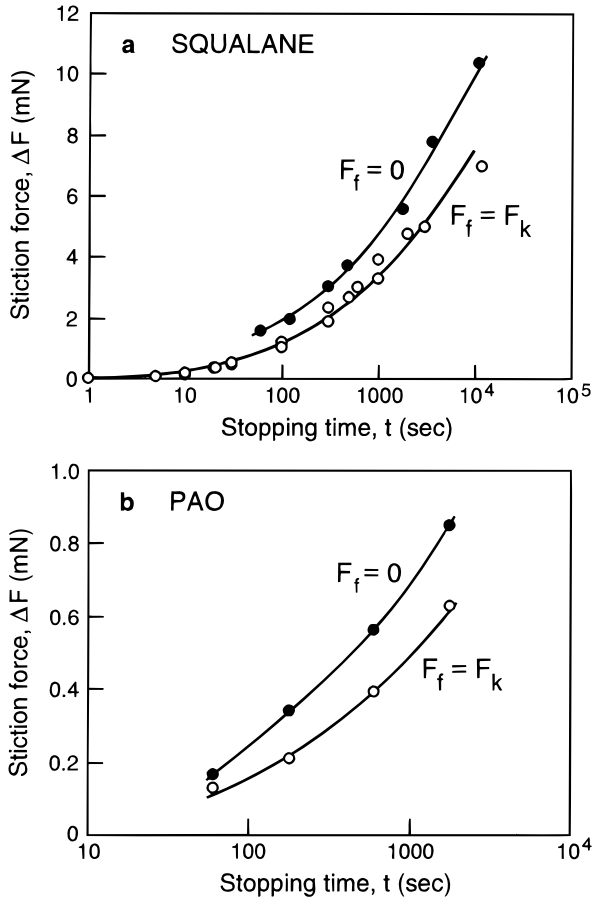

Figure 4. Stiction as a function of waiting time at different resting stresses, F_f. $T = 26$ °C. $V = 0.65$ μm/s. (a) Thin films of squalane. (b) Thin films of PAO.

It is worth mentioning at this point that no significant increase in the area of contact between the atomically smooth surfaces was observed upon aging. Thus, the increase of the static friction force with waiting time seems to be due to configurational changes within the thin films, e.g., to changing intermolecular entanglements and order of the molecules in the films, and not to a creep-induced increase of the contact area. The increase of the "real" area of contact has been the traditional explanation for the increase of the static friction force with contact time in unlubricated, multiple asperity systems,[30−33] but this does not seem to be the explanation for this type of system. Furthermore, the increase in the static friction force is due purely to confinement effects: if the surfaces are kept separated while aging, and brought back into contact just before sliding, no stiction spike is observed, regardless of the contact area.

Evolution to Steady-State Sliding Conditions: Effect of Previous History. We first studied how the films attain steady-state sliding conditions after the initial stiction spike. Thin films of branched hydrocarbons seem to evolve to steady-state sliding in a more complicated fashion than linear hydrocarbons, with spatial and temporal memory effects playing a crucial role in determining the response of these systems under shear. The general behavior observed is presented in Figure 5. Typically, the films need to be sheared for a very long time (or distance) before they reach their steady-state sliding configuration, as gauged from the unchanging friction force. The "transition" to steady-

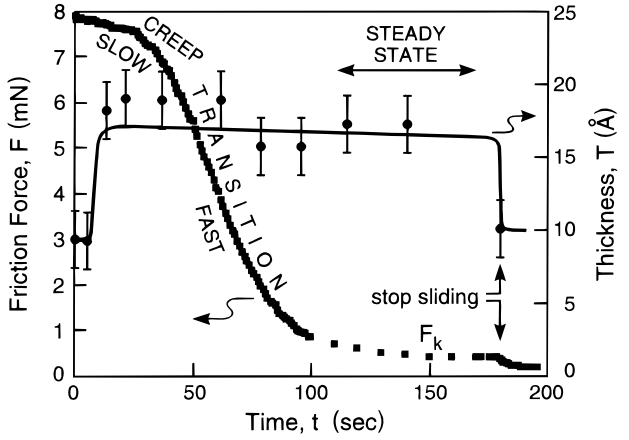

Figure 5. Variations of friction force and film thickness for thin films of squalane undergoing continuous oscillatory shearing. The shear is imposed after keeping the film stationary for 60 min. The film thickness drops very quickly to its original value when shear is stopped. Sliding velocity $V = 83.2$ μm/s, $A_0 = 41.6$ μm, $f = 1$ Hz, $L = 5.6$ mN, and $T = 26$ °C.

state sliding appears to be describable in terms of one or two relaxation times or distances that are much longer than any conceivable molecular length or bulk molecular relaxation time. The fine details of this transition depend on the lubricant used. For squalane, a single-exponential decay was observed at intermediate and high loads (cf. Figure 3b inset). However, for loads smaller than 0.05 mN two clearly differentiated time scales were observed. For PAO, two decay processes were observed at all loads (Figure 3c inset). Exxsyn films displayed less pronounced stiction spikes, with rounded friction force peaks that were preceded by a "creep" regime (Figure 3d inset).

A different situation is observed when steady-state sliding is approached entirely in the "creep" regime, as in the example presented in Figure 5. Such a situation arises, for example, when the lower surface is driven back-and-forth in an oscillatory fashion at constant speed but at an amplitude that never reaches the stiction peak value, F_s. Under such conditions, a slowly varying creep is observed in which the friction force remains initially high and then yields more rapidly to a much lower value with time, as shown in Figure 5. Depending on the experimental conditions of L, T, V, K, and amplitude of oscillation, the slow phase of the "creep transition" can last as long as few hours, being longer at higher loads and lower temperatures. The characteristic time (or distance) of the fast decay to steady-state conditions also depends strongly on load and temperature: the higher the temperature or the lower the load, the shorter the transition time, as can be seen in Figure 6. This slow evolution to steady conditions is never observed for thin films of simple liquids or linear hydrocarbons under shear, where steady-state sliding is reached immediately or after a maximum of few seconds (or microns) of sliding.

An increase in the film thickness is invariably observed just before the friction force begins to fall, i.e., right after the slow phase of the creep regime, as can be observed in Figure 5. This dilatency[34] depends on the sliding velocity and can be very significant at high shear rates, as shown in Figure 7. The refractive index of the film does not seem to change during the process (within the time scales accessible to our experimental setup, i.e., 0.1 s), strongly suggesting that during the dilation fluid

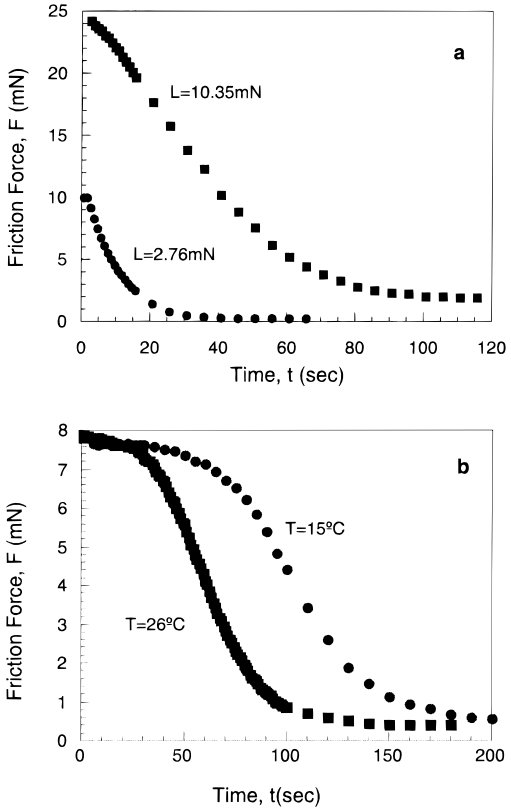

Figure 6. Friction force vs sliding time for thin films of squalane. The shear is imposed at $t = 0$ after a stopping time of (a) 180 min at $T = 26$ °C and (b) 60 min at $L = 5.6$ mN. $V = 83.2$ μm/s.

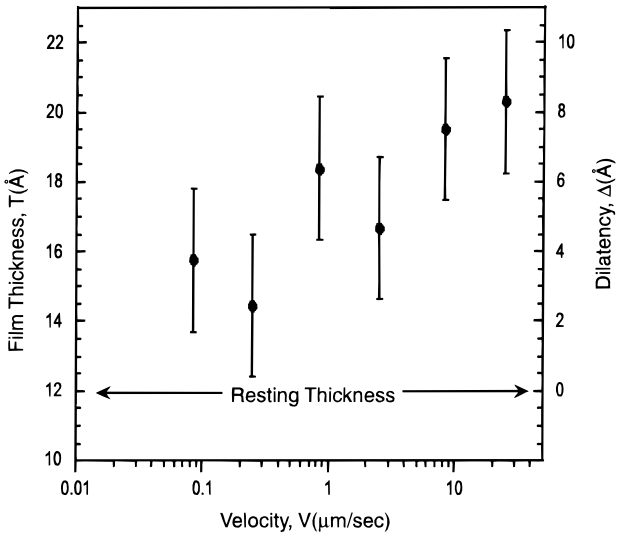

Figure 7. Film thickness as a function of sliding velocity for thin films of squalane. Load = 1.26 mN, $T = 26$ °C.

is flowing into the contact region from the outside reservoir. This effect was not observed with linear hydrocarbon systems, within the experimental resolution. In molecular dynamics simulations of sheared films of short-chained alkanes, Thompson, Robbins, and Grest[8] computed an increasing normal force on the walls accompanied by an increasing film thickness, preceding slip at very high shear rates. A similar dilatency response of hydrocarbon-like chains under shear has been observed in recent computer simulations by other groups studying single asperity contacts.[35,36] A transient change in film thickness during a stick−slip cycle is also

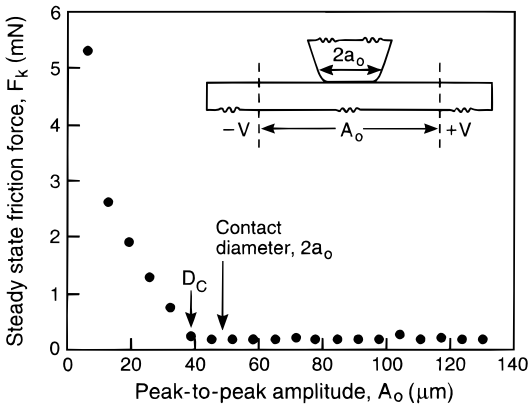

Figure 8. Steady-state friction force vs amplitude of the triangular oscillation A_o of the lower surface for thin films of squalane at $L = 0.33$ mN and $T = 26$ °C. The frequency of the oscillation was changed in order to keep the sliding velocity constant at $V = 0.13$ μm/s.

observed in these simulations, even though it is substantially smaller (strains <10%) than the one observed in here (strains ∼30%). The difference probably arises because of the periodic boundary conditions typically adopted in the computer simulations that impose a constant number density between the walls and thereby eliminates the possibility of material flow/exchange with a reservoir, as we observed in the present experiments.

The slider used for the experiments described so far had a maximum linear displacement of 40 μm, which was of the order of magnitude of the typical contact diameter. The results shown in Figures 5−7 correspond to many back-and-forth oscillations of the slider. From these results and those described in the next section, it became clear that a longer range of *continuous* displacement would prove useful for fully understanding the behavior of complex liquids under shear. For these reasons we built a bimorph slider with a linear range of 500 μm, which allowed us to study in more detail the evolution of thin films to steady-state sliding. The new slider utilizes substantially longer bimorph elements (3 in. long), which allows longer sliding distances without needing to reverse the direction of sliding. As will be described, it was possible to establish the crucial role of the continuous (rather than the total) sliding distance in controlling the evolution of the thin films to steady sliding conditions.

The steady-state value of the friction force was found to be a function of the oscillatory sliding amplitude, even for the same total (cumulative) sliding distance, sliding velocity, and total sliding time. As can be seen in Figure 8, the steady-state friction decreases with sliding amplitude, reaching a constant value only for amplitudes longer than the molecular length, domain size, or even the contact diameter. Even though the sliding velocity was the same for all the data points, the plateau value of the friction force, i.e., the kinetic friction force, strongly depends on how far the surfaces are slid with respect to each other before reversing the shear direction. This provides evidence for the importance of making continuous long-range displacement measurements in any comprehensive investigation of the tribological behavior of fluid lubricants.

Effect of Changes in Sliding Velocity (Shear Rate). The films evolve toward steady state as described above only when the shear rate is the same before and after stopping. If that is not the case, the variation of the shear rate after restarting can be very different depending on the previous history, for example, how long the film is kept at rest. If the sliding velocity is lower after the rest time, a positive slope is obtained for the friction−time curve after the initial stiction spike (if there is one), because the kinetic friction force plateaus at a higher value. This effect is not observed if the films are kept at rest for long periods (>10 min) when the evolution to steady sliding proceeds as described in the previous paragraphs.

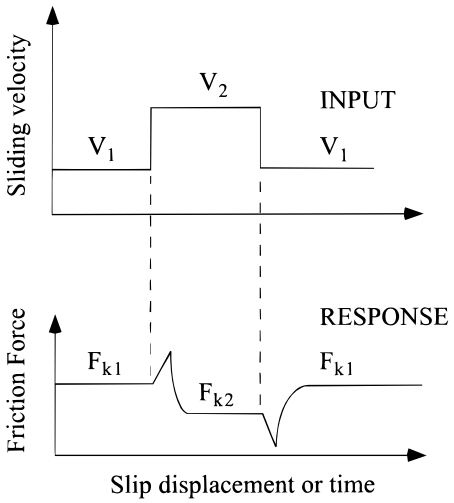

Figure 9. Typical evolution of the friction force at constant normal load. When the sliding velocity is suddenly increased from V_1 to V_2, the friction force increases and then relaxes to the new steady-state value F_{k2}. When the velocity is decreased from V_2 back to V_1, the friction force initially drops and then increases to the original value F_{k1}.

These results indicate that information about the past sliding history persists in the films even after some time at rest. They also suggest that more than one mechanism is involved in determining the magnitude of the static friction force: one process determined by the shear history, and probably associated with the degree of alignment and long-range order of the molecules in the contact area; the other determined by the time at rest under confinement and associated with the local positional ordering and degree of entanglement of the molecules. These different processes are probably related to the different relaxation times observed in the start−stop experiments and are discussed again in the Discussion.

Changing the slope of the voltage ramp being used to drive the bimorph slider (without stopping) imposes an abrupt change of shear rate. The response of the film to a sudden change in V was observed by monitoring the friction force, the area of contact, and the film thickness. In general, it is observed that the friction force evolves to the new steady-state sliding rate in a complicated fashion, with several relaxation processes involved in the transition.

At constant load and temperature the steady-state friction force, F_k, seems to be a function only of sliding velocity. However, we observed that the equilibration time (or distance) required to reach steady state can be very long, as discussed before. Figure 9 is a schematic of what is observed. When the shear rate is suddenly changed, an instantaneous viscous response occurs in the friction force: if the shear rate is increased (decreased), the friction force immediately increases (decreases). This change is then followed by a long time

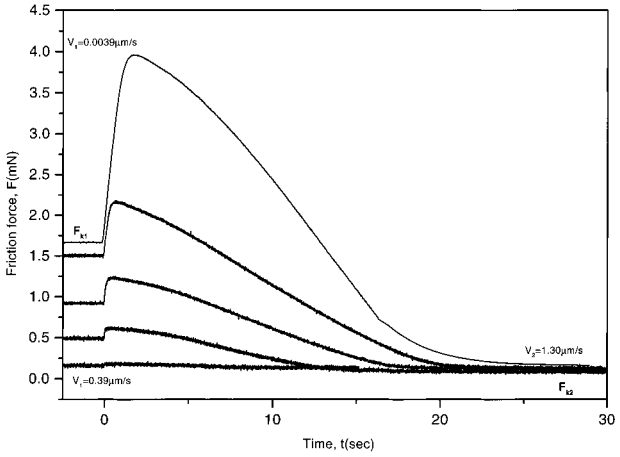

Figure 10. Friction force vs time for thin films of squalane at $L = 0.08$ mN and $T = 26$ °C. At $t = 0$ the sliding velocity is suddenly increased from V_1 to the same final velocity of $V_2 = 1.3$ μm/s. The initial shear rate is, from top to bottom, $V_1 = 0.0039$, 0.013, 0.039, 0.13, and 0.39 μm/s.

evolution of the friction force in the opposite direction toward the new equilibrium value. Dhinojhwala, Cai, and Granick[16] observed a similar behavior for poly(dimethylsiloxane) (PDMS) thin films, but they applied substantially shorter shear amplitudes (<250 nm) and, therefore, could not follow the full evolution of the friction force to continuous steady-state sliding conditions.

The initial stiction-like jump in friction force is strongly dependent on the initial and final sliding velocities, V_1 and V_2, as can be observed in Figure 10. The higher (or lower) the jump in shear rate $|V_2 - V_1|$, the bigger the direct increment (decrement) in the friction force.

In general, a negative value of dF_k/dV (shear thinning) was observed in the range of velocities investigated; however, the value of dF_k/dV seems to plateau at higher loads and lower velocities for films of Exxsyn and PAO, as can be observed in Figure 11. It is possible that the films were still slowly evolving when the data were recorded. It takes a long time, especially at lower velocities, for the films to reach steady-state sliding.

Figures 12a and 13a show the evolution of the friction forces after a sudden increase or decrease in shear rate for thin films of squalane and PAO. It is apparent that longer sliding times are necessary in to reach the steady state when sliding at lower velocities. The same results are presented in Figure 12b and 13b, but now as a function of sliding distance. From the experimental results, it is apparent that the relaxation time increases linearly with the sliding velocity. Figures 12c,d and 13c,d present the same results but now suitably scaled or normalized to further clarify the role of shear distance. In Figure 12c,d the friction force is scaled in such a way that the value of the force is always 1 at the peak. In Figure 13c,d the curves are scaled to coincide at the steady state. It is clear that there is a characteristic distance, not time, that describes the relaxation of the friction force to the steady state. This distance is of the order of the contact diameter, orders of magnitude longer than any typical molecular length. Similar results were obtained with thin films of Exxsyn. These results clearly imply that there exist long-range cooperative processes determining the evolution of the films to the steady state, possibly involving all the molecules in the confined film.

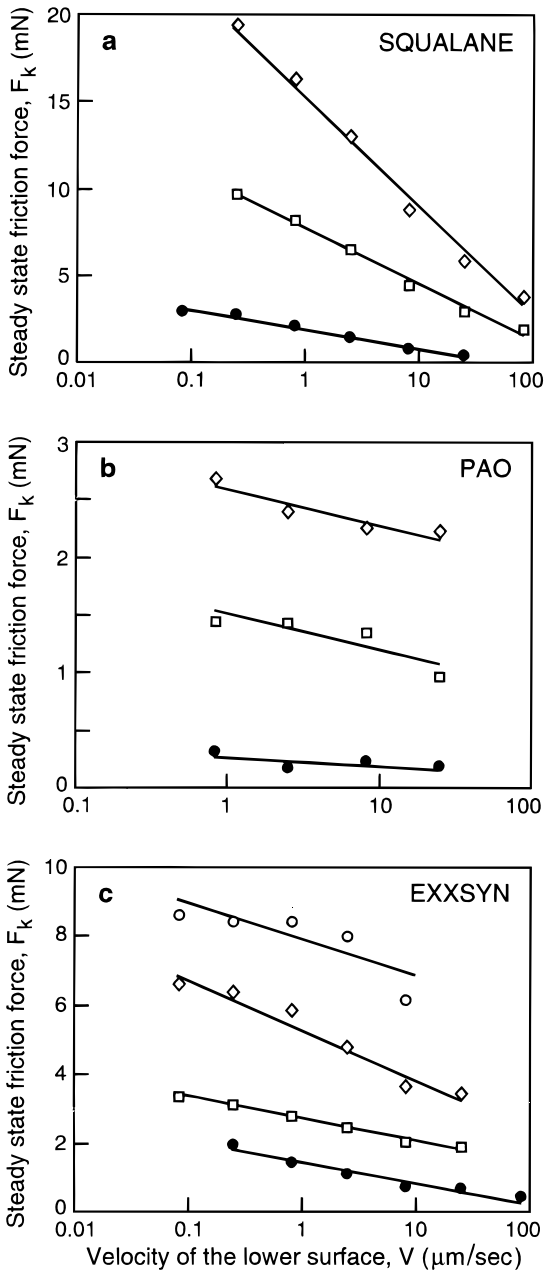

Figure 11. Steady-state friction forces vs sliding velocity at $T = 26$ °C. (a) Squalane. The normal loads are, from top to bottom, $L = 17.94$, 10.35, and 2.76 mN. (b) PAO. The loads are, from top to bottom, $L = 21.32$, 8.95, and 0.73 mN. (c) Exxsyn. The loads are, from top to bottom, $L = 5.62$, 3.78, 1.91, and 0.88 mN.

The observed characteristic distances were in general longer for thin films of Exxsyn and PAO than for squalane. Interestingly, for films of Exxsyn and PAO the transition distances were even larger than the contact size. This implies that the confined molecules must be at least partially dragged with the surfaces (see later), ruling out the possibility of full slip at the surfaces. Otherwise, the population in the contact region would be completely refreshed after sliding farther than the contact diameter, and any further change in the film configuration would be inconceivable.

The evolution of the friction forces described above is always clearly observed with thin films of branched hydrocarbons, but not always—and never as clearly—with linear-chain hydrocarbon films, and is totally absent for short-chained linear hydrocarbons and simple

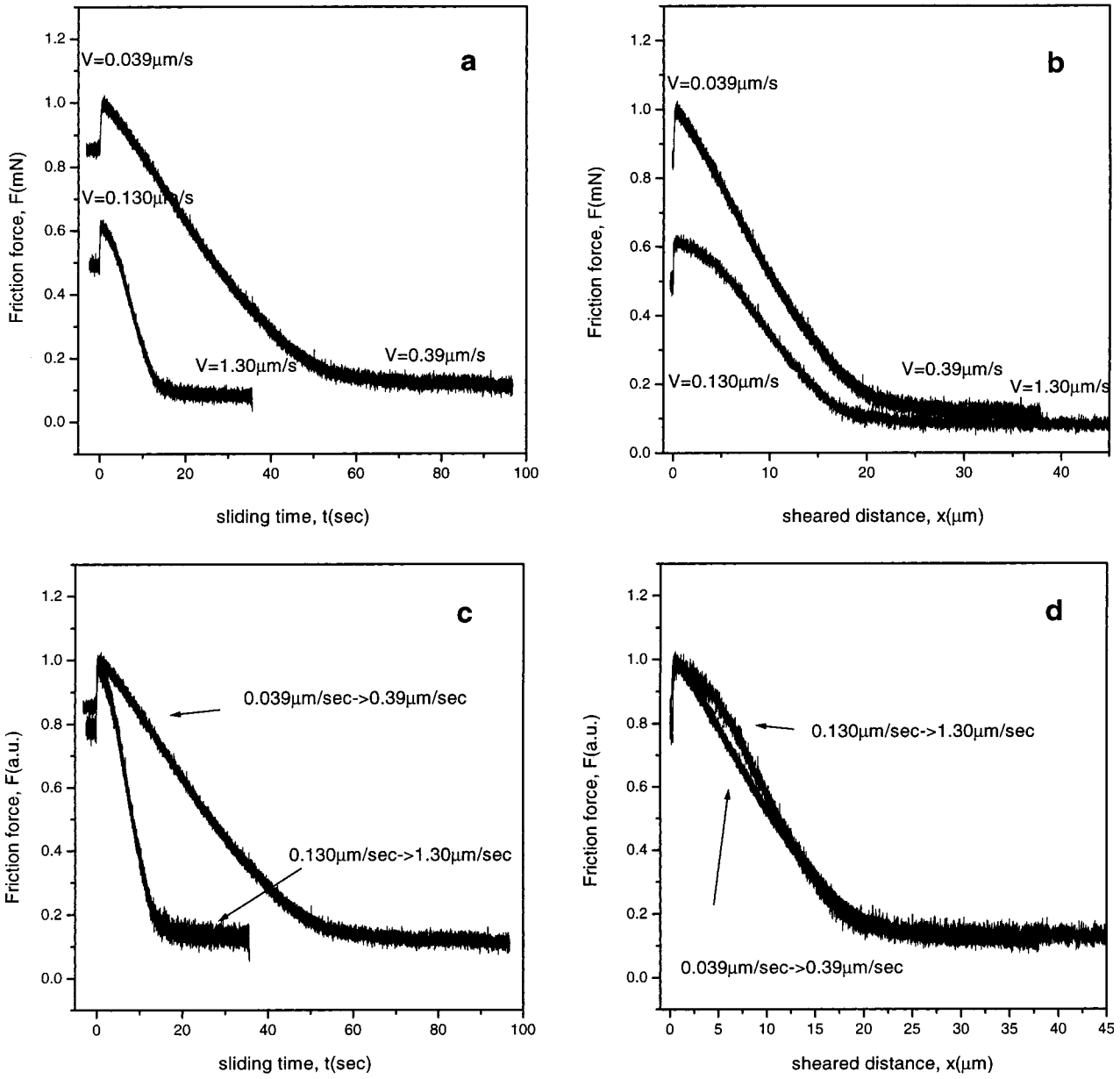

Figure 12. Friction force for squalane thin films at $T = 26$ °C and $L = 0.08$ mN. The sliding velocity is suddenly increased 10-fold from steady sliding. (a) Variation with time for low and high initial velocities. The time origin ($t = 0$) is chosen when the sliding velocity is increased. (b) Same variation of F but plotted against the sliding distance. The position of the origin ($x = 0$) is chosen when the sliding velocity is increased. (c) Same variation with time as in (a) but with both curves scaled to have the value 1 at the peak of the friction force. (d) Same variation with sliding distance as in (b) but with the curves scaled to have the value 1 at $x = 0$.

quasi-spherical molecules. Furthermore, the slip distance necessary to reach steady-state conditions is much longer for branched hydrocarbon films than for films of simpler liquids. A fraction of a micron of sliding suffices to reach steady-state sliding for films of tetradecane or hexadecane; in contrast, it can be necessary to shear branched hydrocarbon thin films for tens of microns (in a continuous fashion) or hundreds of oscillations of a few microns amplitude to achieve the same steady-state. Once again, there is a remarkable difference in characteristic time and/or distance scales between the two systems.

Discussion

The experimental results highlight the importance of considering long time and distance scales when describing the behavior of branched hydrocarbons under shear. Clearly, it is not enough to consider atomic or molecular length scales to describe the tribological behavior of complex fluids lubricants. A description including cooperative phenomena involving many molecules and length scales of the order of and even exceeding the contact size is necessary for a complete description of the experimental observations. Hu and co-workers[8] arrived at similar conclusions from their study of thin films of OMCTS and linear hydrocarbons. They found relaxation times of the order of 0.05 s, which are orders of magnitude longer than any conceivable single-molecule relaxation process. Yoshizawa and Israelachvili[11] also describe a long time evolution to steady-state sliding (of the order of minutes) for thin films of *n*-hexadecane. However, for the films studied in this

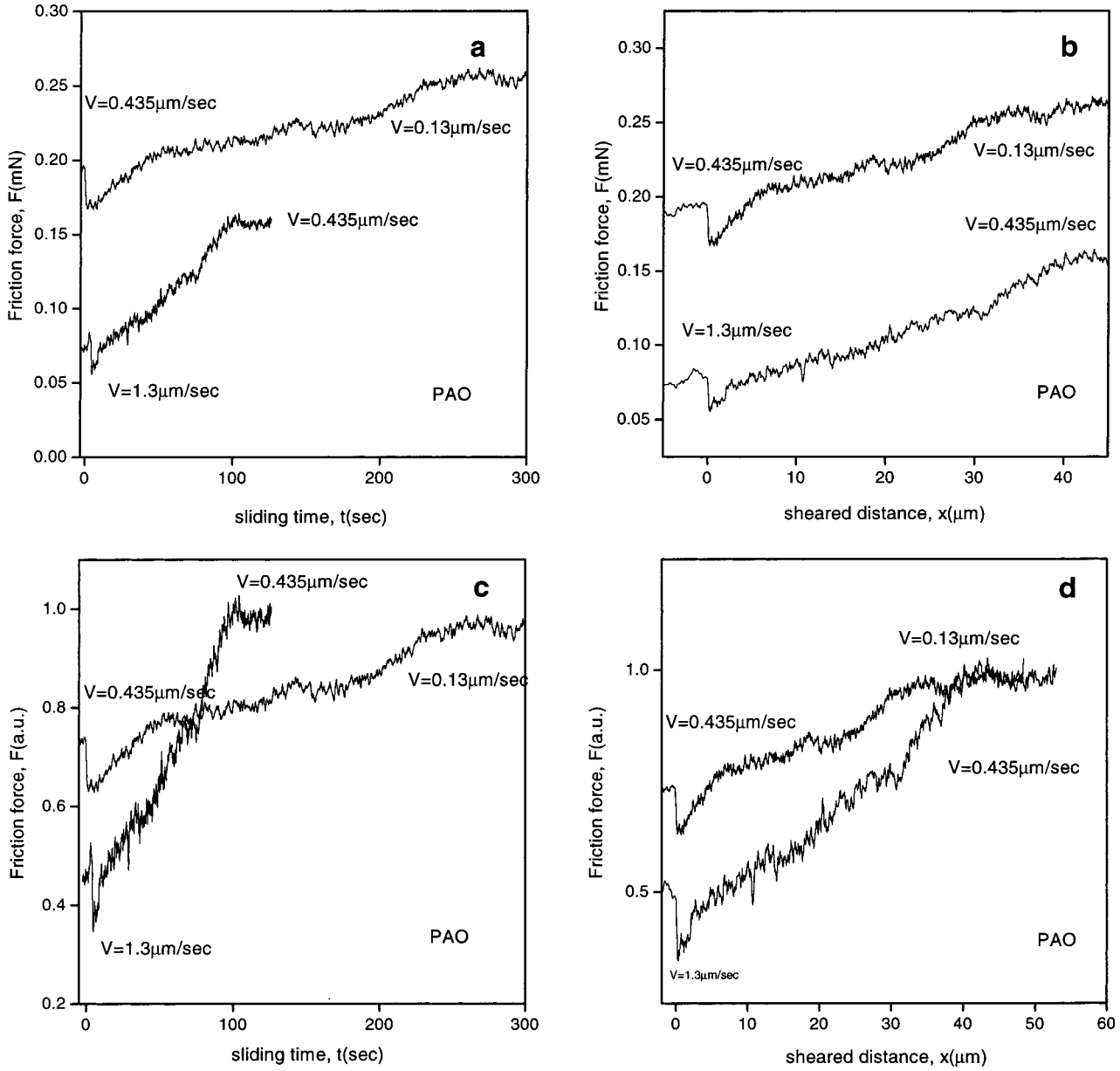

Figure 13. Friction force for PAO thin films at $T = 26$ °C and $L = 0.08$ mN. The sliding velocity is suddenly reduced 3-fold from steady sliding. (a) Variation with time for low and high initial velocities. The time origin ($t = 0$) is chosen when the sliding velocity is decreased. (b) Same variation of F but plotted against the sliding distance. The position of the origin ($x = 0$) is chosen when the sliding velocity is decreased. (c) Same variation with time as in (a) but with both curves scaled to have the value 1 at the steady state. (d) Same variation with sliding distance as in (b) but with the curves scaled to have the value 1 at steady state.

paper even longer relaxation times were observed. As mentioned before, evolution to what appears to be steady-state sliding can take a few hours of constant shearing, especially at small amplitudes or strains, and even after that period, one cannot be certain that the films are still not trapped in a metastable state.

The evolution to steady conditions takes orders of magnitude longer for the films studied in this paper than has been observed before for linear hydrocarbon systems. This should not be surprising: single component and mixtures of branched hydrocarbons should interpenetrate more and show a more complicated spectrum of relaxation processes compared to pure linear hydrocarbons. Linear hydrocarbons have the tendency to align in discrete layers under confinement, as described by Israelachvili and co-workers[37] and computed by Gao et al.[17] using grand canonical ensemble computer simulations. That is not the case for branched hydrocarbons, which also layer under confinement, but where interlayer interdigitation is much more pronounced.[17] Upon shearing, it will be easier to shear-align linear hydrocarbons, because in that case it is not necessary to disentangle a bundle of molecules that are not naturally layered.

All the results described in this paper can be explained, at least at a qualitative level, using a very simple picture of the confined lubricant molecules both inside and outside the contact. This model is presented in Figure 14. When the molecules are first confined (Figure 14a), it is reasonable to assume that they are in a quasi-ordered configuration, but not aligned in any particular in-plane orientation.[38] Extensive grand canonical molecular dynamic simulations by Gao et al.[17] have shown that squalane molecules, unlike linear hydrocarbons, do not arrange in well-differentiated layers under confinement. For that reason, a nonoscil-

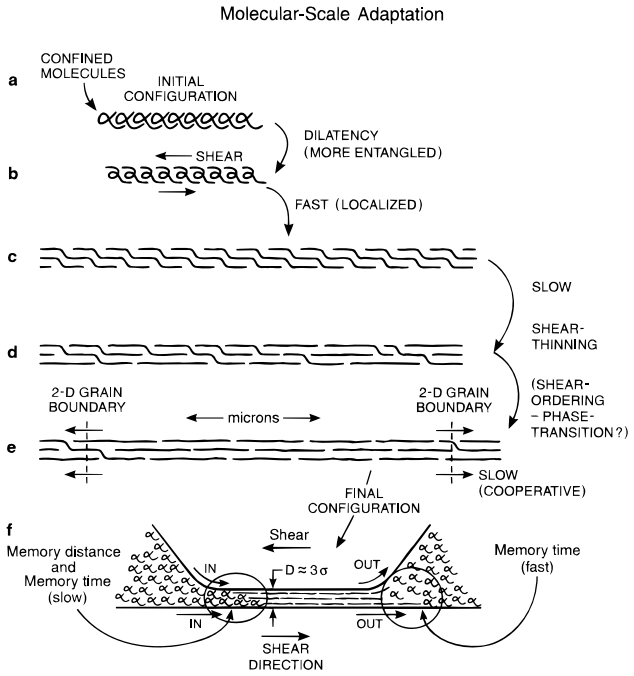

Figure 14. Schematic representation of the film molecules under shear. (a) The lubricant molecules are just confined but not oriented in any particular direction. Because of the need to shear, the film dilates (b). The molecules disentangle (c) and get oriented in a certain direction related to the shear direction (d). (e) Slowly evolving domains grow inside the contact region. These macroscopic domains are responsible for the long relaxation times. (f) At the steady state, a continuous gradient of confinement time and molecular order is established in the contact region which is different for molecules adsorbed on the upper and lower surfaces. Molecules entering into the contact are not oriented or ordered. The required sliding distance to modify their state defines a characteristic distance. Molecules leaving the contact region need some (short) characteristic time to regain their bulk, unconfined configuration.

latory force profile is measured for a thin film of this lubricant between mica surfaces.[12,15,17] It is expected that PAO and Exxsyn would be even more disordered. However, when shear is imposed, the molecules will tend to align (or realign) in some direction related to the shear direction rather than to the crystallographic axes. Our results show that the magnitude of this alignment depends on how fast and for how long (in time and space) the surfaces are slid past each other. The longer the shearing distance, the more a particular molecule inside the contact is "pushed" to align in a particular direction. However, oscillating back and forth over a short distance many times does not have the same effect as sliding over the same total distance continuously in one direction. As a matter of fact, we estimated characteristic sliding distances of the order of thousands of microns, strongly dependent on the sliding velocity, for describing the evolution of squalane films to their steady state when shearing in an oscillatory fashion (at low sliding velocities). For squalane, PAO, and Exxsyn the critical distances D_c for unidirectional sliding were of the order of 10−100 μm, almost independent of shear rate. In contrast, the steady-state configuration for back-and-forth sliding does depend on the amplitude of sliding A_0 when $A_0 < D_c$, as can be inferred from Figure 8 for squalane. This effect is even more important for films of the less symmetric molecules, PAO and Exxsyn. These results show that sheared films can be trapped in metastable states if the shear distance is too small. Recording the friction force solely as a function of velocity, even in the steady state, can therefore be misleading.

At the same time as they are being shear aligned, the confined molecules are also driven to adopt a more disordered configuration because of thermal entropic effects. Nevertheless, the evolution of the molecules to a more disordered state will be slowed significantly because of the confinement, compared with typical relaxation times in bulk. The force necessary to slide the surfaces at a constant shear rate will be a result of the competition between these two opposing effects: on one side, the shear aligning of the molecules to decrease the friction force; on the other side, thermally induced disorder in the film, tending to increase the friction force. It is clear then why the friction forces are higher at lower velocities: the molecules have more time to adopt a more disordered configuration.

Within the context of the model shown in Figure 14, we can consider what will happen when a sudden change in shear rate is imposed after the molecules have attained their steady-state configuration (Figure 14f). Initially the response is expected to be mainly viscous. The force changes in the same direction as the velocity change, as observed in Figures 10, 12, and 13. The molecules need to be slid some distance before adopting the new steady configuration. For this reason, the initial increase (decrease) of the friction force is observed when the velocity is increased (decreased). However, when the molecules in the contact reach the steady-state configuration, a shear thinning effect is clearly observed, as expected from the model described in Figure 14.

Similarly, a steady increase in the static friction force or stiction spike is expected if the surfaces are kept at rest, because of the progressive loss of orientational order of the molecules in the contact and the increasing number of interdigitated segments between them, i.e., going *backward* in Figure 14.

In general, the responses of these systems to changes in shear rate show striking similarities to those reported for unlubricated, multiple asperity systems of polymer,[28] rock,[25,26] and paper surfaces.[27] Most of the models attempting to explain the behavior of those rough surfaces are based on the fact that they are multiple asperity systems and that the area and lifetime of each contact change with time.[30−33] In that regard, the stop−start experiments and the tribological response to changes in shear rate are two manifestations of the same phenomena which can be described in terms of rate-and-state models, with state variables that are related to the "real" area of contact and the "age" of the contacts.[30−33] In light of our results, it seems reasonable that there exist more fundamental reasons for the observed behavior in both kinds of systems, which involve changes *within* the contact areas (or films). Is the "real area of contact" a valid (or even useful) concept? Even though the surfaces used in this experiment are completely free of steps or irregularities, it is not *necessarily* true that there is "action" all along the surfaces simultaneously. It is conceivable that there exist different scenarios in different places at different times in the contact region: different domains contributing differently to the total friction force—sliding in some places and sticking in others. In that sense, even the atomically flat contacts used in these experiments would constitute a rough system at the molecular level.

Currently we are trying to determine whether the similarities between friction in dry rough surfaces and in surfaces lubricated with branched hydrocarbons can be extended beyond the qualitative analogy that was presented in this paper. Rate-and-state models, which have proven to be extremely successful in quantitative describing dry friction behavior, could improve our understanding of the dynamics of confined lubricants under shear.

Conclusions

The following conclusions can be drawn from our results:

(i) The dynamical response under shear is more complicated for branched hydrocarbons than for linear hydrocarbon thin films, with long memory effects—in both time and space—playing a very important role determining the evolution of the friction forces to steady-state sliding. The friction force is thus not a function of the instantaneous sliding velocity but of the previous history of the sheared film, especially the continuous sliding distance. In addition, there is no simple scaling between microscopic and macroscopic contacts or of fast and slow time scales in lubricated tribological systems.

(ii) A velocity-dependent increase in film thickness (dilatency), which involves material flow into the contact, was observed soon after subjecting the films to a shear stress but before the surfaces started to move significantly.

(iii) The frictional response of molecularly smooth single asperity systems lubricated with thin films of branched hydrocarbon fluids displays many similarities with rough, unlubricated, plastically deformable, multiple-asperity systems reported in the past, suggesting the existence of a broadband spectrum of relaxation processes occurring in single asperity films even when they are atomically smooth and of uniform thickness throughout the contact area.

(iv) Highly complex structural rearrangements and slip conditions are likely to be occurring during sliding that are different in different parts of the same trapped film. The existence of large distance or length scales, D_c, should not be construed as *necessarily* reflecting the existence of large molecular domains within the films. Rather, they may be a reflection of the "massaging distance" that surfaces need to be stroked or the number of times N they need to be hit by passing molecules of size σ (where $D_c = N\sigma$), before they adapt to the steady state.

Acknowledgment. This work was funded by grants from INTEVEP S.A., Venezuela, Exxon Research and Engineering Company, NJ, and the Department of Energy under Grant DE-FG03-87ER45331.

References and Notes

(1) Dowson, D. *History of Tribology*; Langman: London, 1979.
(2) Israelachvili, J. N. *Surf. Sci. Rep.* **1992**, *14*, 109 and references therein.
(3) Mate, C. M.; McClelland, G. M.; Erlandsson, R.; Chiang, S. *Phys. Rev. Lett.* 1**987**, *59*, 1942. Erlandsson, R.; Hadziioannou, G.; Mate, C. M.; McClelland, G. M.; Chiang, S. *J. Chem. Phys.* 1**988**, *89*, 5190.
(4) Krim, J.; Widom, A. *Phys. Rev. B* 1**988**, *38*, 12184.
(5) Harrison, J. A.; Brenner, D. W. In *Handbook of Micro/Nano Tribology*; Bhushan, B., Ed.; CRC Press: Boca Raton, FL, 1995 and references therein.
(6) Horn, R.; Israelachvili, J. *J. Chem. Phys.* **1981**, *75*, 1400. Klein, J.; Kumacheva, E. *Science* 1**995**, *269*, 816. Demirel, A. L.; Granick, S. *Phys. Rev. Lett.* 1**996**, *77*, 2261.
(7) Israelachvili, J.; McGuiggan, P.; Gee, M.; Homola, A.; Robbins, M.; Thompson, P. *J. Phys.: Condens. Matter* 1**990**, *2*, SA89.
(8) Hu, H.-W.; Carson, G. A.; Granick, S. *Phys. Rev. Lett.* 1**991**, *66*, 2758.
(9) Thompson, P. A.; Robbins, M. O.; Grest, G. S. *Isr. J. Chem.* 1**995**, *35*, 93.
(10) Klein, J.; Kumacheva, E. *J. Chem. Phys.* 1**998**, *108*, 6996.
(11) Yoshizawa, H.; Israelachvili, J. *J. Phys. Chem.* 1**993**, *97*, 11300.
(12) Gee, M. L.; McGuiggan, P. M.; Israelachvili, J. *J. Chem. Phys.* **1990**, *93*, 1895.
(13) Yoshizawa, H.; Chen, Y.-L.; Israelachvili, J. *Wear* **1993**, *168*, 161.
(14) Luengo, G.; Schmitt, F.-J.; Hill, R.; Israelachvili, J. *Macromolecules* 1**997**, *30*, 2482.
(15) Granick, S.; Demirel, A. L.; Cai, L. L.; Peanasky, J. *Isr. J. Chem.* 1**995**, *35*, 75.
(16) Dhinogwala, A.; Cai, L.; Granick, S. *Langmuir* 1**996**, *12*, 4537.
(17) Gao, J.; Luedtke, W. D.; Landman, U. *J. Chem. Phys.* 1**997**, *106*, 4309. Gao, J.; Luedtke, W. D.; Landman, U. *Phys. Rev. Lett.* 1**997**, *79*, 705.
(18) Wang, Y.; Hill, K.; Harris, J. G. *J. Chem. Phys.* 1**994**, *100*, 3276.
(19) Stevens, M. J.; Mondello, M.; Grest, G. S.; Cui, S. T.; Cochran, H. D.; Cummings, P. T. *J. Chem. Phys.* 1**997**, *106*, 7303.
(20) Homola, A. M.; Israelachvili, J. N.; Gee, M. L.; McGuiggan, P. M. *J. Tribol.* 1**989**, *111*, 675.
(21) Israelachvili, J. *J. Colloid Interface Sci.*1**973**, *44*, 259. Heuberger, M.; Luengo, G.; Israelachvili, J. *Langmuir* 1**997**, *13*, 3839.
(22) Berman, A. D.; Ducker, W. A.; Israelachvili, J. N. *Langmuir* 1**996**, *12*, 4559.
(23) Carlson, J.; Berman, A. Manuscript in preparation.
(24) Yamada, S.; Israelachvili, J. *J. Phys. Chem.* 1**998**, *102*, 234.
(25) Dieterich, J. H. *J. Geophys. Res.* 1**979**, *84* (B5), 2161.
(26) Rice, J. R.; Ruina, A. L. *J. Appl. Mech.* 1**983**, *50*, 343.
(27) Baumberger, T.; Heslot, F.; Perring, B. *Nature* 1**994**, *367*, 544. Heslot, F.; Baumberger, T.; Perrin, B.; Caroli, B.; Caroli, C. *Phys Rev. E* 1**994**, *49*, 4973.
(28) Berthoud, P.; Baumberger, T.; G'Sell, C.; Hiver, J.-M. *Phys Rev. B* 1**999**, *59*, 14313.
(29) Hirz, S.; Subbotin, A.; Frank, C.; Hadziioannou, G. *Macromolecules* 1**996**, *29*, 3970.
(30) Scholz, C. H.; Engleder, J. T. *Int. J. Rock Mech. Sci. Geomech. Abstr.* 1**976**, *13*, 149.
(31) Teufel, L. W.; Logan, J. M. *Pure Appl. Geophys.* 1**978**, *116*, 840.
(32) Dieterich, J. H. *Pure Appl. Geophys.* 1**978**, *116*, 790.
(33) Brockley, C. A.; Davis, H. R. *J. Lubr. Technol.* 1**968**, *90*, 35.
(34) We mean by dilatency an increase of the film thickness induced by shear. In these experiments the process is accompanied by material flow into the contact.
(35) Batista, A. A., private communication.
(36) Bajon, A. R. C.; Robbins, M. O. In *Micro/Nanotribology and Its Applications*; Bhushan, B., Ed.; Kluwer Academic Publishers: Dordrecht, 1997.
(37) Israelachvili, J.; Kott, S. J.; Gee, M. L.; Witten, T. A. *Macromolecules* 1**989**, *22*, 4247.
(38) Confinement alone is known to induce positional ordering and layering of chain molecules between surfaces. However, there is no preferred direction of the aligned molecules other than determined by the surface lattices.

MA9919918